Inhomogeneously Polarized Laser Modes

V.G. Niziev
Institute on Laser and Information Technologies Russian Academy of Sciences,
140700, Shatura, Russia, niziev@laser.ru

Introduction

The radiation of the majority of modern lasers is homogeneously polarized. Ellipsometric parameters of radiation are the same in all points of the cross section of a laser beam. The field distribution over a cross section of laser beam is described by the solution of the scalar wave equation [1].

However there is a big class of solutions of the vector wave equation presented inhomogeneously polarized modes (IPM) with unique physical properties.

The modes with radial and azimuthal polarization are the most interesting from the practical point of view because they have full axial symmetry of all the beam parameters including polarization. This property is often useful for applications.

There are two main conceptions to obtaining an inhomogeneously polarized mode IPM: internal-cavity and external-cavity techniques.

Among different intra-cavity methods of generation of such modes the diffractive mirrors with high local polarization selectivity take a particular place. The special groove drawing ensures maximum quality for a definite mode, for example with azimuthal polarization. Other modes will be depressed having substantial intra-cavity losses. This method is optimal for high power lasers, like CO_2-lasers. Such lasers have high gain of active media, low quality of resonator and relatively low quality of radiation.

Out-of-resonator methods of IPM formation are based on the coherent superposition of two usual modes TEM_{p1} (p=0, 1, 2…) with the help of an interferometer. An external cavity technique can be effectively used for lasers with a short wavelength, low gain and high resonator quality. The space and temporal coherence is much higher in such lasers than in high power lasers. These "high quality modes" can interact coherently outside the resonator.

This report presents the review of the last achievements in description and generation of laser modes with axially symmetric polarization.

1. Theoretical description of laser beams with axially symmetric polarization.

The pictures presented in Fig. 1 are widely known. They schematically explain the principle of formation of IPM, radially and azimuthally polarized beams [2].

However the description of IPM following this scheme by using the classic solutions for Laguerre-Gaussian modes is not resulting. The principal difficulties on this way are connected with serious inner contradictions of classic solutions not acceptable for analysis of IPM.

It is known well that the classic solutions are in the state of contradiction with Maxwell equation $\nabla \mathbf{E}=0$ [3]. It makes impossible to determine formally boundaries of applicability of such approximation. They also neglect the longitudinal component of field. It is not a direct consequence of paraxial approximation; it is an additional restriction of the theory.

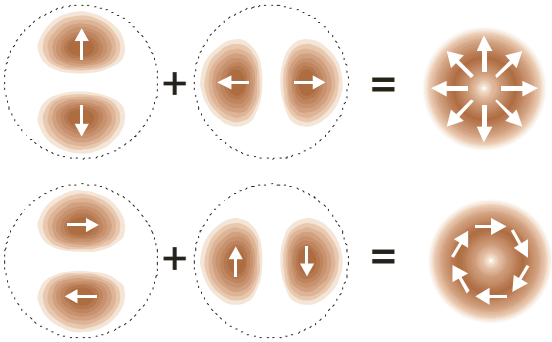

Fig.1. Generation of radially and azimuthally polarized modes as a result of superposition of two linearly polarized modes TEM_{01}.

1.1. Paraxial approximation in cylinder coordinates.

Let us consider the radially or azimuthally polarized beams offering the most interesting cases of inhomogeneously polarized modes. A method of theoretical description of the radially or azimuthally polarized beams is presented that excludes any inherent contradictions and unjustified approximations.

A solution will be sought in the class of azimuthally polarized modes. It has been proved in [4] that the condition of radial or azimuthal polarization automatically results in the axial symmetry of field

amplitude distribution. Represent the desired function in the form $\mathbf{H}=H_\varphi(r,z)\cdot\mathbf{e}_\varphi(\varphi)$. The equation $\nabla\mathbf{E}=0$ in this case is satisfied, and the vector wave equation is reduced to the scalar type:

$$\frac{1}{r}\frac{\partial}{\partial r}r\frac{\partial H_\varphi}{\partial r}+\frac{\partial^2 H_\varphi}{\partial z^2}+\left(k^2-\frac{1}{r^2}\right)H_\varphi=0$$

The solution of the last equation in paraxial approximation is r-z part of expression for Laguerre-Gaussian modes TEM_{pq} at q=1.

$$H_\varphi=\sqrt{\frac{2p!}{\pi(p+1)!}}\cdot\frac{1}{w}\cdot\left(\sqrt{2}\cdot R\right)\cdot L_p^1\left(2\cdot R^2\right)\cdot\exp\left(-R^2\right)\cdot\exp(i\theta) \tag{1}$$

$$\theta=2\mathrm{arctg}Z-2Z\frac{z_0^2}{w_0^2}-ZR^2;\quad R=r/w;\quad R_0=r/w0;\quad Z=z/z_0;\quad z_0=\frac{\pi w_0^2}{\lambda};$$

$$w^2=w_0^2\cdot\left(1+Z^2\right)$$

$$L_p^1(x)=\sum_{m=0}^{p}(-1)^m\frac{(p+1)!}{(p-m)!\,(m+1)!\,m!}x^m$$

The electric field components E_r and E_z are determined through Maxwell equation $\nabla\times\mathbf{H}=-ik\mathbf{E}$. These analytical expressions are quite cumbersome, so they will be written only for the beam waist of z=0.

$$E_r\approx H_\varphi=\frac{2}{\sqrt{\pi}}\frac{1}{\sqrt{p+1}}\frac{1}{w_0}R_0L_p^1\left(2\cdot R_0^2\right)\exp\left(-R_0^2\right) \tag{2}$$

$$E_z=i\frac{1}{\pi\sqrt{\pi}}\frac{\lambda}{w_0}\frac{1}{w_0}\sqrt{(p+1)}\exp\left(-R_0^2\right)\left[L_p(2R_0^2)+L_{p+1}(2R_0^2)\right] \tag{3}$$

An approximate equality of E_r and H_φ takes place under the condition $\frac{\lambda^2}{\pi^2 w_0^2}<<1$.

The presented method of calculation for the mode with azimuthally directed field can not be formally used for the fields of radial direction. In fact, the representation of the field in the form of $\mathbf{H}=H_r(r,z)\cdot\mathbf{e}_r(\varphi)$ is contrary to the equation $\nabla\mathbf{H}=0$. Physically this means that the azimuthally polarized mode (in the absence of other components of the same field) is available, but the mode with purely radial direction of the field does not exist. The presented method permits the field components to be calculated for two classes of modes:

$\mathbf{H}=H_\varphi(r,z)\cdot\mathbf{e}_\varphi(\varphi)$, $\mathbf{E}=E_r(r,z)\cdot\mathbf{e}_r(\varphi)+E_z(r,z)\cdot\mathbf{e}_z$.
$\mathbf{E}=E_\varphi(r,z)\cdot\mathbf{e}_\varphi(\varphi)$, $\mathbf{H}=H_r(r,z)\cdot\mathbf{e}_r(\varphi)+H_z(r,z)\cdot\mathbf{e}_z$

The set of two equations: the wave equation and $\nabla\mathbf{E}=0$ is additive. This means, in particular, that the superposition of such modes with arbitrary complex coefficients also corresponds to Maxwell equations.

1.2. Longitudinal component of field

One of the most interesting phenomena connected with inhomogeneously polarized laser beams is the longitudinal component of the electric field in the focal spot of lens. This direction of field is in contradiction with transverse nature of electromagnetic wave. It is interesting from the physical point of view, because the energy associated with this component is not transmitted. The classical solution for homogeneously polarized mode cannot be used directly for calculation of the longitudinal component of field just following to pictures like Fig. 1 for radially polarized mode. Classical solutions neglect the longitudinal component and they are in contradiction with Maxwell equation $\nabla\mathbf{E}=0$. Nevertheless, in IPM at sharp focusing this neglecting is unjustified both physically and mathematically. The reason is that the longitudinal component of the field has its maximum amplitude in the places where the "common" component of the field is zero. Despite the lack of deep insight into the physical nature of this component of the field, the first experiments have been run on its registration [5, 6]. The suggestions for practical application of this component have also been made. At sharp focusing the longitudinal component of electric field can be used in acceleration of relativist electrons [7, 8].

Analysis of these formulas gives several character features of this field component parallel to wave vector.

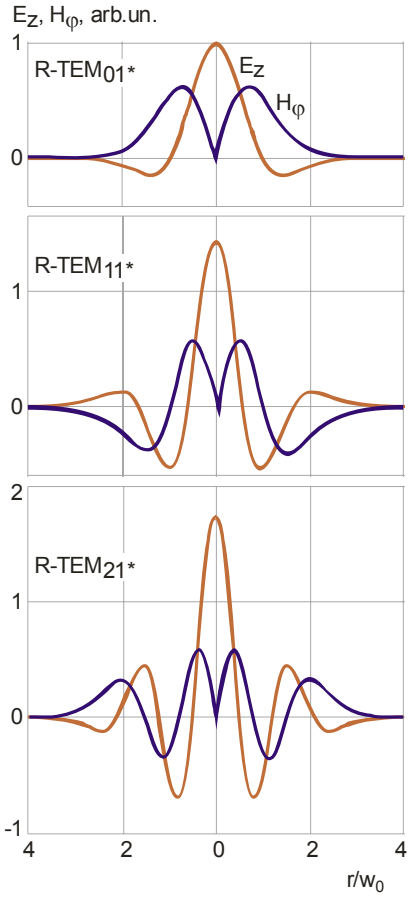

Fig.2. Calculated distributions of longitudinal component of electric field E_z and azimuthal component of magnetic field H_φ in the waist of radially polarized modes of different order.

1. The maximum of this field is on the beam axis, where magnetic field and radial component of electric field equal to zero.
2. This field has additional efficient λ/w_0 in comparison with H_φ и E_r.
3. The imaginary unit in E_z means this field component changes in time with quarter wavelength phase shift with respect to magnetic field. This leads to time averaged Pointing vector connected with this component equals to zero. The energy connected with E_z is not transmitted,

The explanation of the fact that the impossibility of this component transfer is due to the absence of magnetic field at the beam axis, which is found in the literature, is inexact. The magnetic field and the longitudinal component of electric field offer the overlapping radial distributions, though, in accordance with the derived expression, at all the points of the beam cross section in its waist the time averaged Pointing vector associated with longitudinal component of the field equals zero.

Fig. 2 presents the distributions of H_φ and E_z for the radially polarized modes R-TEM$_{p1*}$ with p=0, 1, 2.

1.3. Debye approximation for sharp focusing

The calculation procedure under consideration should be extended to Debye approximation: the method of field calculation in the lens focal plane [9-12]. The calculation of distribution for the azimuthally polarized component does not display any inherent contradictions, the calculation results are in agreement with Maxwell equation $\nabla\mathbf{E}=0$. The solution obtained the magnetic field $H_\varphi(r, z)$, for example, allows the calculation of the radial and longitudinal components of the electric field:

$$E_r = \frac{1}{ik}\frac{\partial H_\varphi}{\partial z};\quad E_z = i\frac{1}{kr}\frac{\partial\left(rH_\varphi\right)}{\partial r}.$$

Expressions for components of fields in this case are:

$$H_\varphi(r,z) = k\int_0^{\theta_1} H_{\varphi 0}\left(f\sin\alpha\right)\sqrt{\cos\alpha}\ J_1(k\rho\sin\alpha)\exp(ikz\cos\alpha)\sin\alpha\,d\alpha$$

$$E_r(r,z) = k\int_0^{\theta_1} H_{\varphi 0}\left(f\sin\alpha\right)\sqrt{\cos\alpha}\ J_1(k\rho\ \sin\alpha)\exp(ikz\ \cos\alpha)\sin\alpha\cos\alpha\,d\alpha \qquad (4)$$

$$E_z(r,z) = -i\cdot k\int_0^{\theta_1} H_{\varphi 0}\left(f\sin\alpha\right)\sqrt{\cos\alpha}\ J_0(k\rho\ \sin\alpha)\exp(ikz\ \cos\alpha)\sin\alpha^2\,d\alpha\,d\beta$$

Here θ_1 is the angle determined by beam aperture and focal length of a lens. The field distribution in the waist corresponds to z=0. The analogous formulas can be written for the other field components: $E_\varphi(r,z)$, $H_r(r,z)$, $H_z(r,z)$. In this case we can take the electric field with azimuthal polarization $E_{\varphi 0}(r)$ as an initial field. The use of Debye approximation for plane or radial polarization leads to formal contradiction with equation $\nabla\mathbf{E}=0$.

Consider the peculiarities of coherent composition of two counter-propagating beams producing a standing wave. For definiteness, take the perfectly identical counter-propagating beams with zero phase

shift. The azimuthally polarized fields $H_\varphi(r, z)$ appear oppositely directed, and the resulting field is described by the expression $H_\varphi(r, z)-H_\varphi(r,-z)$. Further, Maxwell equations are applied to find the electric field components E_r and E_z. For the standing wave the following expressions are derived:

$$\begin{aligned} H_\varphi(r,z) &= 2ik\int_0^{\theta_1} H_{\varphi 0}(f\sin\alpha)\sqrt{\cos\alpha}\ J_1(k\rho\sin\alpha)\sin(kz\cos\alpha)\sin\alpha\, d\alpha \\ E_r(r,z) &= 2k\int_0^{\theta_1} H_{\varphi 0}(f\sin\alpha)\sqrt{\cos\alpha}\ J_1(k\rho\ \sin\alpha)\cos(k\,z\ \cos\alpha)\sin\alpha\cos\alpha\ d\alpha \\ E_z &= -2k\int_0^{\theta_1} H_{\varphi 0}(f\sin\alpha)\sqrt{\cos\alpha}\ J_0(k\rho\sin\alpha)\sin(kz\cos\alpha)(\sin\alpha)^2\, d\alpha \end{aligned} \qquad (5)$$

It is evident that in the waist z=0 we have the nodes of standing wave for the components of the fields H_φ and E_z, and for the E_r component an antinode is generated (E_r is always zero on the beam axis). A unique situation has emerged when all the three components of field are zero at the coordinate origin. This feature will be discussed in detail in the following section.

The conditions for realization of standing waves are typically ensured in the optical resonators with the aligned reflective mirrors which facilitate the generation of counter-propagating fluxes of radiation. In the case of standing wave the energy is not transferred for the transverse component of the field as well. However, in the case of the transverse component of electric field the physical reason for this phenomenon is quite different than for the longitudinal component. The longitudinal component of field that can not transfer the energy exists both in the traveling and standing waves.

It is of interest to follow the relationship of phases in the field components for the traveling and standing waves. First consider a traveling wave. Let the time dependence be presented as $H_\varphi \sim \sin(\omega t)$. Then, according to formulae (4), with regard to phase relationships, $E_r \sim \sin(\omega t)$, and $E_z \sim \cos(\omega t)$. Where the amplitudes of fields are not zero, the product of H_φ and E_r, averaged in time, is not zero, which means the energy transfer in the direction of wave vector. Nevertheless, the product of H_φ and E_z is proportional to $\sin(2\omega t)$, and averaging in time results in zero irrespective of the amplitudes of these fields.

In the standing wave, the formulas (5), we have the following functions of time: $H_\varphi \sim \sin(\omega t)$, $E_r \sim \cos(\omega t)$, $E_z \sim \cos(\omega t)$. It means the absence of the time averaged energy transfer for both field components E_r and E_z. It is valid for the any points.

2. The methods of generation of beams with axially symmetric polarization.

Two main forms for conception to obtaining IPM are internal-cavity and external-cavity techniques. One of the internal-cavity techniques uses a diffractive mirror as one of resonator mirrors. It is preferable for lasers with high gain in the active media and low resonator quality.

An external-cavity technique can be effectively used for lasers with a short wavelength, low gain and high resonator quality. The mode quality in such lasers is much higher than in high power lasers. These “high quality modes” can therefore interact coherently outside the resonator.

The results of generation of IPM with the help of Sagnac interferometer are presented below.

2.1. Diffractive mirrors for intra-cavity method of generation of IPM.

The property of polarization selectivity for diffraction grating has long been known. For example the diffraction grating itself and technology of its manufacturing were described in details in [13]. They proposed to use this diffraction grating as a beam splitter.

Another idea is to use such an optical component to ensure definite direction of plane polarization of laser beam. For this purpose the diffraction grating with metal coating and groove period d=12μm was installed in the industrial CO_2-laser. The radiation came to the grating surface normally. The degree of polarization 98.5% at the output power 2.3 kW was achieved.

The same grove parameters and technology of manufacturing as in [14] were used in the experiments of [15], but drawing of groves was adopted for the generation of radially polarized radiation. This diffractive mirror was used as the rear mirror of laser resonator.

The diffractive mirrors were made by the photolithography and wet etching method. The reflectivity of the wave was $\rho_{\|}$=94% (if the vector of electric field is parallel to grooves) and $\rho_{\perp}$ = 72% (if the vector of electric field is perpendicular to grooves). There is the comparison of two diffractive mirrors in the table.

		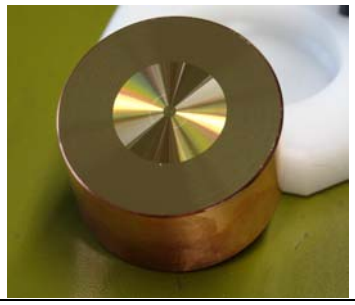
Year of production	2000	2006
Manufacturer	ILIT RAS, Russia	II-VI, USA
Technology	Photolithography, wet etching copper	Diamond turning, gold coating
Reflectivity, $E_{\perp}$-$E_{\parallel}$	94% - 72%	94% - 20%
Price	-----	~ $1000

2.2. Generation of inhomogeneously polarized laser beams using a Sagnac interferometer

The main advantage of this method is its universality. It can be applied for any wavelength and for any type of IPM.

A Melles Griot He–Ne laser with output power of 6.0 mW was used. This laser has a tube with a sealed Brewster window at one end and a mirror at the other. The mode TEM_{01} with a controlled direction of plane polarization can be selected through the aperture. The mutual orientation of the mode pattern and the electric field vector can be changed by rotating the $\lambda/2$ phase shifter. A beam expander increases the beam diameter for convenience.

We used a Sagnac interferometer in our experiments. An attractive feature of the Sagnac interferometer is that both the interfering beams sample the same optical path with the same elements, so distortions of the optics have a minimal effect on the sensitivity of the differential signal [16, 17]. A simplified scheme of a Sagnac interferometer, which is based on standard optical components, is presented in Fig. 3a.

The intensity distribution of two split beams can be mutually rotated by inserting a Dove prism (DP), as seen in Fig. 3b. The spatial orientation of the intensity distributions of the beams in plane F just after the lateral displacement polarizing beam splitter is absolutely the same. Then each beam passes the DP and an angle reflector (AR) in different sequence and comes to the lateral displacement beam splitter, which works now as a combiner. If both elements of the DP and AR have the same orientation in space, their common effect of rotating the beam intensity distribution will be zero. If the DP and AR possess a mutual orientation, as shown in Fig. 3c, $\theta=22.5°$, the intensity distribution of each two beams will be rotated around the beam axis in opposite directions at an angle of $2\theta=45°$ so that the total mutual rotation angle is $4\theta=90°$.

Four $\lambda/2$ phase shifters were installed in this scheme in the places indicated by arrows. PS1 was used for correction of amplitudes of two beams after splitting. Correction was performed by rotating PS1 around the beam axis. The axes of the second and third PS are parallel each other and oriented at an angle $\beta=10.25°$ along the bisector of the angle θ between the DP and AR as shown in Fig. 4. These phase shifters are necessary to avoid changes of polarization made by the Dove prism. The beam polarization at the entrance and exit of the subsystem consisting of the three optical components (DP, PS2 and PS3) will be the same.

The fourth PS was used for correcting a phase shift between two interfering beams on the beam combiner. The axis of this PS must be parallel ($\gamma=0°$) or perpendicular ($\gamma=90°$) to the AR edge. The correction of phase shift is performed by turning the PS around the line, which is perpendicular to the plane of drawing in Fig. 3. Fig. 5 shows the corresponding setup mounting on the optical table.

The modes with radial and azimuthal directions of the electric field are only two representatives of the large family of inhomogeneously polarized modes that are solutions of the vector wave equation. Some of them are presented in Fig. 6. They can be obtained with the help of the suggested scheme. The experimental results of the typical diagnostics of radially and azimuthally polarized beams are presented in Fig. 6. The reconstructed beam from a Sagnac interferometer has a ring-type distribution of intensity (Fig. 7a). This beam passes through a polarizer-analyzer and the resulting picture is fixed on the screen. The Fig. 7b shows the experimental pictures for a mode indicated in Fig. 6e. The single difference between the mode in Fig. 6e and a radially polarized mode consists in a phase shift between two mode patterns combined at the exit of the interferometer. The diagnostically obtained pictures for a radially polarized beam are presented in Fig. 7c.

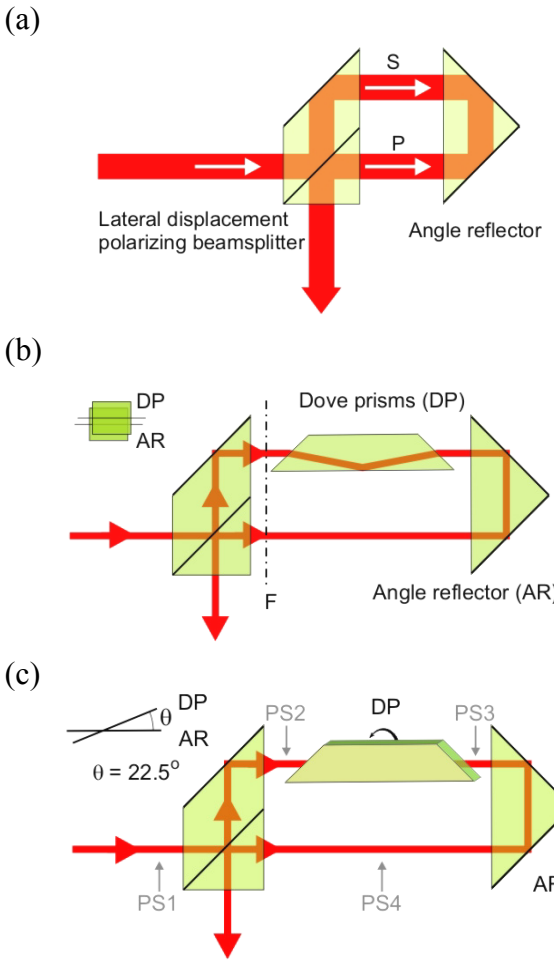

Fig.3. The scheme of a Sagnac interferometer. The simplified scheme (a); P and S are the corresponding polarization of two beams. The scheme with a Dove prism (b). The modified Sagnac interferometer configuration to produce laser beams with inhomogeneous polarization (c).

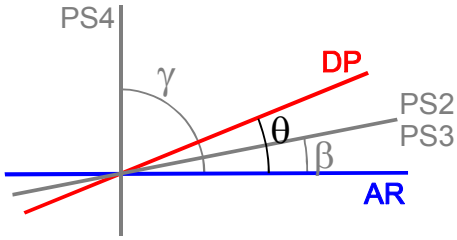

Fig.4. Graphical explanation concerning installation of half-wavelength phase shifters into experimental setup, where $\beta = 10.25°$, $\gamma = 90°$, and $\theta = 22.5°$

The suggested scheme based on a Sagnac interferometer is simple and inherently stable. This scheme has one beam exit and high efficiency of beam transformation.

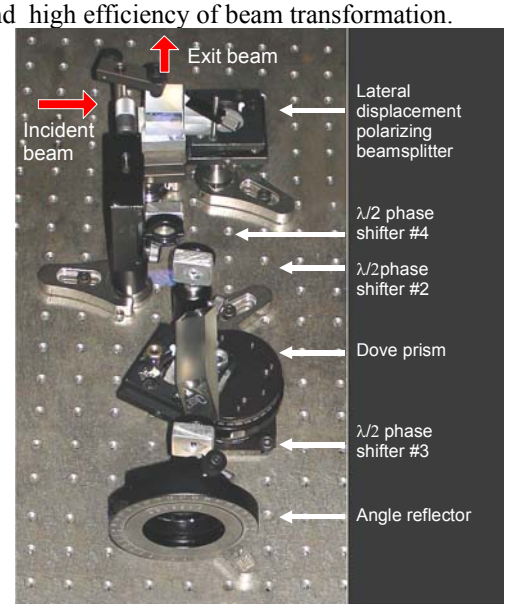

Fig.5. Modernized Sagnac interferometer mounted on the optical table.

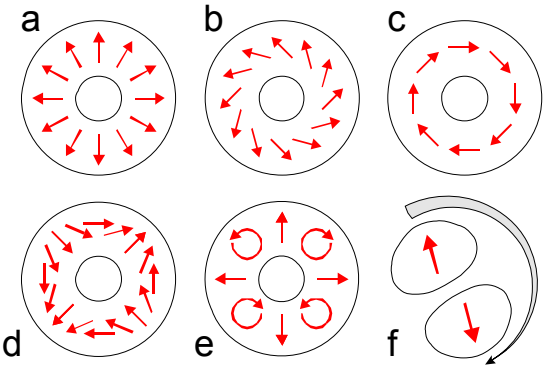

Fig.6. Several examples of inhomogeneously polarized resonator modes. a) The radially polarized mode R-TEM$_{01*}$. b) The angle between **E** and radius is 45°. c) The azimuthally polarized mode A-TEM$_{01*}$. d) The mode with different direction of electric field. e) The mode with different type of polarization. f) Helical mode with plane polarization.

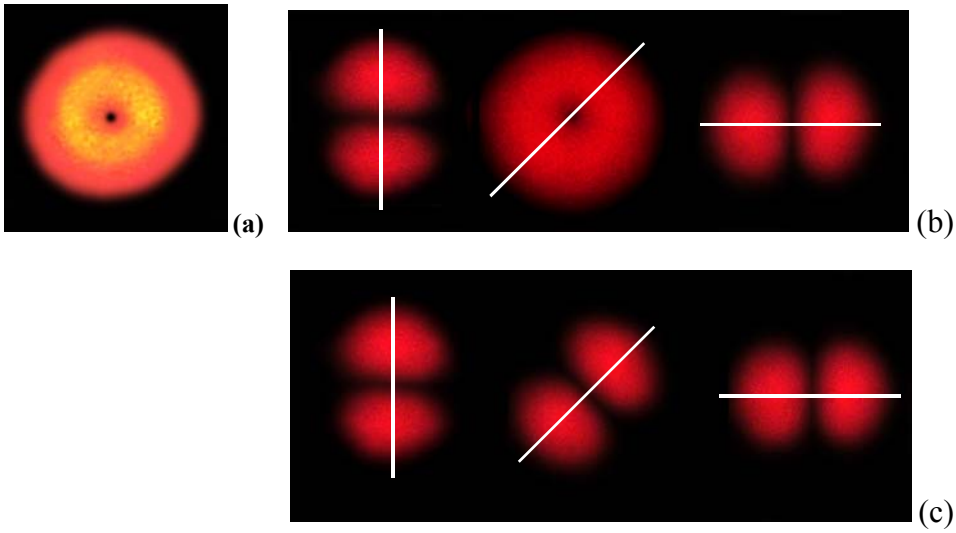

Fig.7. Experimentally obtained pictures of the modes with axially symmetric polarization. a) Intensity distribution in the cross section of the laser beam. b) The diagnostics of the mode with inhomogeneous polarization indicated in Fig. 6e. The intensity distribution is just after the polarizer-analyzer. The white line is the axis of the polarizer. c) The diagnostics the radially polarized beam indicated in Fig. 6a. The white line is the axis of the polarizer. The mode pattern rotates with rotation of a polarizer around the beam axis.

3. Spherical modes

A case of spherical mode will be considered which is of physical interest as a limit situation of sharp focusing. We have here the same circumstances as in examination of laser beams in the cylindrical coordinates. As in the previous case, a solution will be sought in the class of azimuthally polarized modes under the axial symmetry of the distribution of field amplitude $\mathbf{H}=H_\varphi(r,\theta)\cdot\mathbf{e}_\varphi$. The equation $\nabla\mathbf{E}=0$ is in this case satisfied, and the vector wave equation is reduced to the scalar one:

$$\frac{1}{r^2}\frac{\partial}{\partial r}\left(r^2\frac{\partial H_\varphi}{\partial r}\right)+\frac{1}{r^2\sin\theta}\frac{\partial}{\partial\theta}\left(\sin\theta\frac{\partial H_\varphi}{\partial\theta}\right)-\frac{H_\varphi}{r^2\sin\theta}+k^2H_\varphi=0$$

The common solution of this equation is:

$$H_\varphi(r,\theta)=\mathrm{Const}.P_n^1(\cos\theta)\cdot j_n(kr) \qquad (6)$$

P_n^1 - the associated Legendre polynomials.

j_n – The spherical Bessel function of the first kind. At the choice of this function the expression describes standing wave resulting from superposition converging and diverging waves.

The components of electric field are found from the equation $\nabla\times\mathbf{H}=ik\mathbf{E}$:

$$E_r(r,\theta) = -Ci\, n(n+1) P_n(\cos\theta) j_n(kr) \frac{1}{kr} \tag{7}$$

$$E_\theta(r,\theta) = -Ci\, P_n^1(\cos\theta) \left[\frac{n+1}{2n+1} j_{n-1}(kr) - \frac{n}{2n+1} j_{n+1}(kr) \right] \tag{8}$$

Here $P_n = P_n^0$. Let's calculate the energy flux through a sphere:

$$P_{rad} = c_{light} \int_0^\pi 2\pi (r\sin\theta) \cdot \left(E_\theta^2(r,\theta) + H_\varphi^2(r,\theta) \right) \cdot (r\, d\theta),$$

using a well-known expression:

$$\int_{-1}^{1} \left[P_n^1(x) \right]^2 dx = \frac{n(n+1)}{2n+1}$$

This permits the calculation of the constant in our expressions for the components of fields of any order modes provided that the energy flux is permanent.

$$P_{rad} = 2\pi \frac{C^2}{k^2} c_{light} \frac{n(n+1)}{2n+1}$$

The field energy associated with the non-propagating component of the field *** can be found by volume integration:

$$W_{non} = \int_0^\pi \int_0^\infty 2\pi r^2 \sin\theta \left[E_r(r,\theta) \right]^2 d\theta\, dr$$

It is clear from the physical consideration that all the three components of the field H_φ, E_r, and E_θ must be zero in the centre of the sphere, which imposes a restriction on the choice of mode order n=2, 3, 4…. The Pointing vector calculated with regard to the components H_φ, E_θ is radially directed, and it defines the convergent and divergent waves. The field E_r is non-radiating. The polar angle distributions of the fields are determined by the corresponding Legendre polynomials and are shown in Fig. 8. It should be noted that the number of lobes in the distribution of the fields H_φ, E_r, and E_θ is increased with the number of mode, though the spatial localization of these components is different. The field E_r of maximal amplitude is localized at the poles, while the components H_φ, E_θ on the polar axis are, naturally, zero.

The radial dependences of the field components H_φ, E_r and E_θ are illustrated by Fig. 9.

The scales of two curves on the figures are different for n=2 and n=16. They were so chosen that the maximal amplitudes of the fields were much the same. This was done in order to emphasize an important qualitative peculiarity of the distributions under consideration. The radius of the zero field zone is increased with the mode number for the three field components. Recall that this significant result has been obtained from the solutions corresponding to Maxwell equations. This behavior of the fields implies that the field of higher-order modes does not reach the centre of the sphere. The convergent wave of the field possessing such a structure is "reflected" from the sphere having the radius of the order of n/k.

Another qualitative feature of the presented distributions is that the longitudinal field is radially decreased faster that the components H_φ and E_θ. The expression for the field amplitude contains an additional multiplier 1/kr. In practice, it means that the longitudinal field is located in some "spherical shell" of the radius and thickness growing with the mode number. This is evident from the outline drawings of the modes of different orders (Fig. 10).

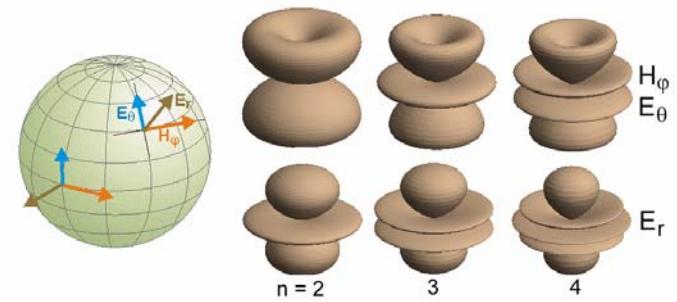

Fig.8. The distribution of field components H_φ, E_r, E_θ in coordinates: azimuthal angle – polar angle for spherical modes of the different order.

Fig. 11 illustrates the variation of the amplitudes of three components of the fields at the maximum as a function of the order of mode. The calculations were performed using the formulae with the coefficients for the permanent flowing of radiating energy from the sphere. All the three curves have been plotted on a single matched scale. The location of the maximums of the field components in the coordinates θ, r is displayed in Fig. 10. The coordinate r_{max} corresponding to the maximum value of the field for all the components H_φ, E_r and E_θ is determined from the simple formula $kr_{max} \approx n$. The maximum of the non-radiating field is always found at $\theta_{max} = 0$. For the components H_φ, E_θ $\theta_{max} = 45°$ at n=2 and tends to zero as n grows.

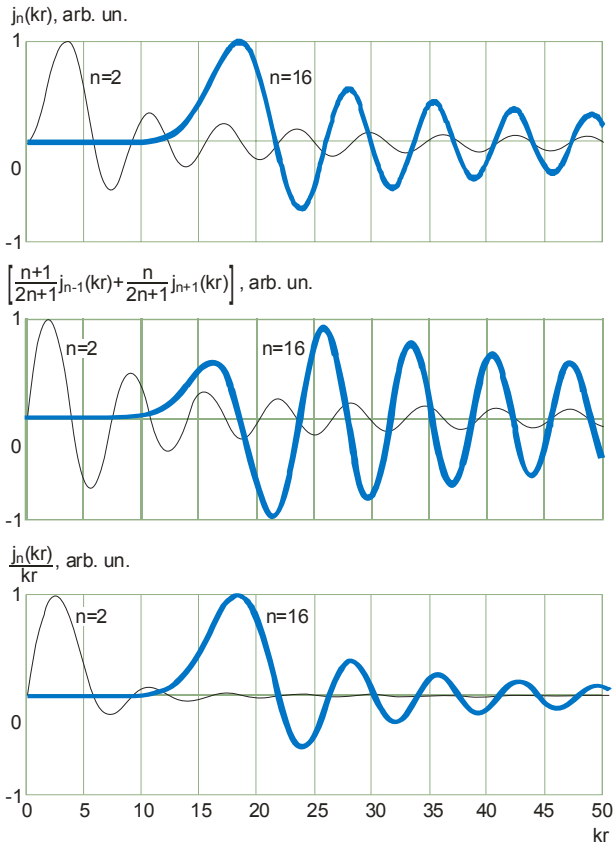

Fig.9. The radial dependence of field components H_φ, E_θ, E_r for the modes of different order.

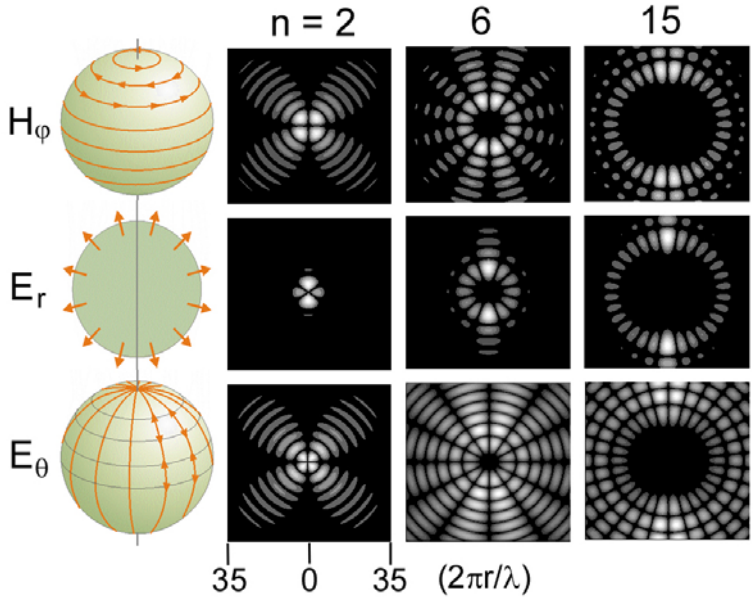

Fig.10. The distribution of field components H_φ, E_r, E_θ in coordinates: radius – polar angle for spherical modes of the different order.

We have given a consideration to the problem in the following order: finding the magnetic field H_φ, calculating the components of the electric field E_r, E_θ. Of course, the problem can be solved "in the reverse direction", i.e. find the azimuthally directed electric field E_φ and then calculate the components of the magnetic field H_r, H_θ which will produce a mode with an "opposite orientation of fields". Here, as in the first case, Maxwell equation $\nabla\mathbf{E}=0$ is satisfied. The magnetic field directed along the radius H_r is in this case a "non-propagating component".

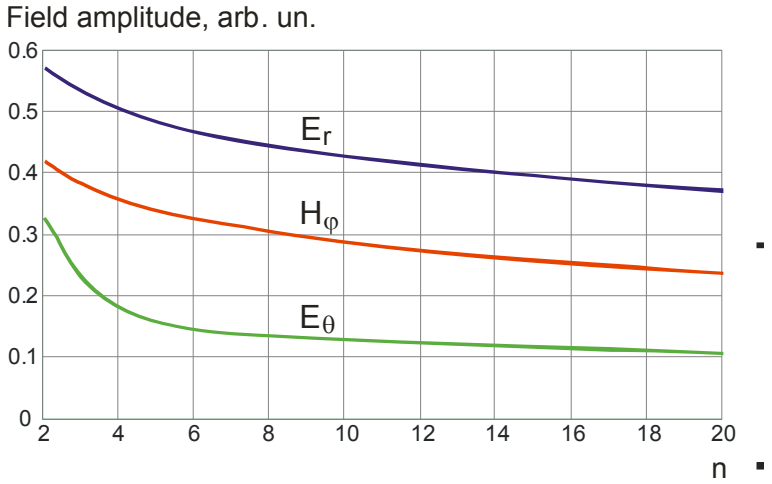

Fig.11. The amplitude of field components H_φ, E_r, E_θ in maximum, as a function of mode order.

Conclusion

A method has been suggested for description of the azimuthally and radially polarized modes that excludes any inherent contradictions and unjustified approximations, as happens with the scalar theory of Laguerre-Gaussian modes. The solutions in the class of azimuthally polarized modes with the axial symmetry of field distribution are in accordance with Maxwell equation $\nabla\mathbf{E}=0$, and the wave equation is reduced to a scalar form. This allowed the analytical calculation of the field components for these modes, including the longitudinal one. The longitudinal field displays a time phase shift, so the energy associated with this field is not transferred. The formulae of field distribution at sharp focusing are presented for the arbitrary-order IPM.

The paper analyzes the evolution of diffraction mirrors used in generation of IPM in high-power CO_2 lasers. For the lasers of low power the out-of-resonator vector superposition of usual TEM_{p1} (p=0, 1, 2…) modes by using of a Sagnac interferometer offers a promising scheme. This method is remarkable for its high efficiency, stability and universality. The paper reports the experimental results on this scheme.

The calculation of the higher-order spherical modes yielded the original results. The centre of a sphere has a particular zone, the diameter of which is increased with the growth of mode order. All the components of electric and magnetic fields in this zone are zero.

References

1. S. Solimeno, B. Crosignani, P. DiPorto, "Guiding, Diffraction and Confinement of Optical Radiation", Academic Press, New York, 1986.
2. Pressley R.J. (ed) Handbook of Laser with Selected Data on Optical Technology, Cleveland: Chemical Rubber Company, 1971,.
3. M, Lax, W. Louisell and W. Mc Knight, From Maxwell to paraxial wave optics Phys. Rev. A 11 1365–70, 1975.
4. A.V. Nesterov, V. G. Niziev, "Laser Beams with Axially Symmetric Polarization," J. of Phys. D: Appl. Phys. 33, 1817-1822, 2000.
5. R. Dorn, S. Quabis, And G. Leuchs, "Sharper Focus for a Radially Polarized Light Beam," Phys. Rev. Lett. 91, 233901, 2003.
6. G. Miyaji, N. Miyanaga, K. Tsubakimoto, K. Sueda, and K. Ohbayashi Intense longitudinal electric fields generated from transverse electromagnetic waves Applied Physics Letters 84, 19 p.3855-3857, 2004.

7. S. C. Tidwell, D. H. Ford, W. D. Kimura, “Generating Radially Polarized Beams Interferometrically,” Appl. Opt. 29, 2234-2239, 1990.
8. S. C. Tidwell, G. H. Kim, W. D. Kimura, “Efficient Radially Polarized Laser Beam Generation with a Double Interferometer,” Appl. Opt. 32, 5222-5229, 1993.
9. A.V. Nesterov, V. G. Niziev, “Propagation Features of Beams with Axially Symmetric Polarization,” J. Opt. B: Quantum and Semiclassical Opt. 3, 215-219, 2001.
10. J. Stamnes Waves in Focal Regions The Adam Hilger Series on Optics and Optoelectronics Bristol: Institute of Physics Publishing, 1986.
11. S. Quabis, R.Dorn, M. Eberler, O. Glöckl, G. Leuchs The focus of light – theoretical calculations and experimental tomographic reconstruction. Appl. Phys. B 72, 109-113, 2001.
12. Yuichi Kozawa nd Shunichi Sato Focusing Properties of a double-ring-shaped radially polarized beam Optics Letters 31, 6, p. 820-822, 2006.
13. H. Haidner, P. Kipfel, J. Sheridan, J. Schwider, N. Strebl, J. Lindolf, M. Collischon, A. Lang, J. Hutfiess «Polarizing reflection grating beamsplitter for the 10.6 mm wavelength» Optical Engineering" v.32, n.8, p.1860, 1991.
14. Jakunin V., Balykina E., Manankova G., Novikova L., Seminogov V. Diffraction polarizing mirror for resonators of high power CO2-lasers. Proc. of the VIth International conference «Laser Technology ‘98» (ILLA’98), Shatura: NICTL-RAN, p. 60, 1998
15. A.V. Nesterov, V. G. Niziev, V. P. Yakunin, “Generation of High-Power Radially Polarized Beam” J. of Phys. D: Appl. Phys. 32, 2871-2875, 1999.
16. P. T. Beyersdorf, M. M. Fejer, K. L. Byer, “Polarization Sagnac interferometer with postmodulation for gravitational-wave detection,” Opt. Lett. 24, 1112-1114, 1999.
17. J. Hwang, M. M. Fejer, W. E. Moerner, “Scanning interferometric microscopy for the detection of ultrasmall phase shifts in condensed matter,” Phys. Rev. A 73, 021802(R), 2006.